Available online at www.sciencedirect.com
SCIENCE DIRECT®
PERGAMON
Polyhedron 22 (2003) 1617–1625
POLYHEDRON
www.elsevier.com/locate/poly

Non-planar manganese Schiff-base complexes; synthesis and molecular structures

Christopher J. Sanders, Paul N. O'Shaughnessy, Peter Scott *

Department of Chemistry, University of Warwick, Coventry CV4 7AL, UK

Received 14 February 2003; accepted 9 April 2003

Abstract

The reactions of anhydrous sodium salts of three chiral biaryl-bridged salicylaldimine tetradentate proligands H_2L with manganese(II) chloride give the corresponding solvated complexes [$Mn^{II}L$]. The molecular structure of one chiral nonracemic example with a relatively low steric demand ligand set is shown to be composed of a homochiral dimer with bridging phenoxy groups. Both LMn units adopt the *cis*-β structure with Δ helicity as predetermined by the (*R*)-configuration of the biaryls. Oxidation of these compounds with halogens gives manganese(III) complexes. A complex [Mn^{III}LI] has a trigonal bipyramidal structure with similar *cis*-β structure to that above. In contrast, the complex [$MnL(OH_2)_2$]Cl has the rather rare C_2-symmetric *cis*-α structure. It is thus apparent then that while the biaryl unit in these and similar compounds is able to predetermine the chirality-at-metal very efficiently, it is quite possible for conversions between diastereomeric forms *cis*-β and *cis*-α, albeit with the same helicity, to occur in response to the nature of the co-ligands.

Keywords: Manganese; Epoxidation; Biaryl; Schiff-base; Chiral-at-metal

1. Introduction

Catalysts based on complexes of chiral salen ligands (e.g. **I**) for the epoxidation of unfunctionalised alkenes, and other important processes [1] have essentially planar *trans* structures (Fig. 1). We and others have developed biaryl Schiff-base ligands [2] such as L^n and closely related binaphthyls [3,4] which give non-planar architectures of the C_2-symmetric *cis*-α and C_1-symmetric *cis*-β classes.

These latter systems have an element of chirality arising from the helicity of the ligand arrangement about the metal. Most importantly, the biaryl backbone directs the helicity of the complex such that usually only a single diastereomer[1] (i.e. one of the four *cis*-α and *cis*-β structures) is formed. This is a good example of predetermination of chirality-at-metal [5]. These systems are, in principle, well-suited for application to enantio-

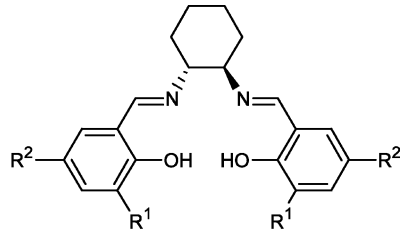

"cysalen"

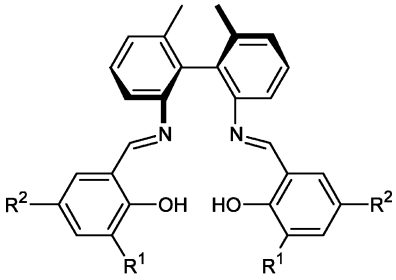

H_2L^1 $R^1 = R^2 = Bu^t$
H_2L^2 $R^1 = H$, $R^2 = Bu^t$
H_2L^3 $R^1 = R^2 = Cl$

* Corresponding author. Fax: +44-24-7657-2710.
E-mail address: peter.scott@warwick.ac.uk (P. Scott).

[1] Or pair of diastereomers in the case of racemic samples.

0277-5387/03/$ - see front matter
doi:10.1016/S0277-5387(03)00285-7

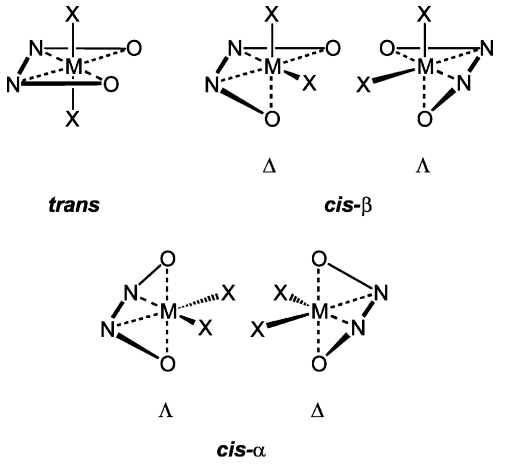

Fig. 1. Stereochemical descriptors for N_2O_2 Schiff-base complexes at octahedral centres. For the biaryl and binaphthyl systems such as L^n, the (*R*)-configured biaryl directs the complexes to have Δ helicity.

selective catalysis; two mutually *cis* coordination sites are formed at which stereoselective reactions can be mediated under the potent influence of the well-expressed chiral-at-metal architecture. Indeed, we have recently reported a ruthenium(II) complex which gives extremely high diastereoselectivity ($\leq$99:1) and enantioselectivity ($\leq$98%) in catalytic alkene cyclopropanation [2g]. Excellent enantioselectivities in the trimethylsilylcyanation of aldehydes using a titanium binaphthyl Schiff-base complex have also been reported [4c]. For alkene epoxidation however using *e.g.* manganese complexes of such ligands, enantioselectivities and catalyst productivity have been disappointing in comparison to the conventional planar Schiff-bases [3,4b]. During this work however we have synthesised a number of complexes of manganese(II) and (III) with ligands of the type L^n. The molecular structures obtained cast further light on the issue of preferred orientations (Fig. 1) in these and related systems in that, for example, both the (expected) *cis*-β structure and the rare *cis*-α structure have been observed, depending on the co-ligature.

2. Experimental

Unless stated otherwise, procedures were carried out under an inert atmosphere of argon by using a dual manifold vacuum/argon line and standard Schlenk techniques, or in an MBraun glove box. All solvents were dried by refluxing for three days under dinitrogen over the appropriate drying agents (sodium for toluene; potassium for THF and benzene; sodium–potassium alloy for diethyl ether, petroleum ether and pentane; calcium hydride for dichloromethane and acetonitrile) and degassed before use. Solvents were stored in glass ampoules in the dark under argon. All glassware, cannulae and Celite were stored in an oven (>100 °C) and flame dried immediately prior to use. Most reagents and chemicals were purchased from either Aldrich Chemical company or Acros Chemical company and used without further purification. Deuterated solvents were freeze-thaw degassed and dried by refluxing over potassium (or calcium hydride for CD_2Cl_2) before being vacuum distilled to a clean, dry Young's tap ampoule and being stored in the glove box. Deuterated chloroform was dried in the bottle in air over molecular sieves (4 Å).

NMR spectra were recorded on Bruker DPX-300 and DPX-400 spectrometers and the spectra were referenced internally using residual protio solvent resonances relative to tetramethylsilane ($\delta = 0$ ppm). Mass spectra were measured using a Micromass Autospec. Infrared spectra were obtained either as Nujol mulls or by evaporation of dichloromethane solutions onto IR plates, using Perkin-Elmer FTIR spectrometer. Elemental analyses were performed by Warwick Analytical Services on a Leeman Labs CE-440 analyser. Magnetic susceptibility measurements were made on a Johnson Matthey balance. 2,2′-Diamino-6,6′-dimethylbiphenyl [2j] and H_2L^1 proligand [2c] were synthesised as previously reported.

2.1. (±)-H_2L^2

(±)-2,2′-Diamino-6,6′-dimethylbiphenyl (1.4 g, 6.5 mmol) and 5-*tert*-butylsalicylaldehyde (2.3 g, 13.1 mmol) were dissolved in methanol (50 ml) stirred under reflux for 5 h to produce a bright yellow crystalline solid. The reaction mixture was cooled to -30 °C before the Schiff-base was isolated by vacuum filtration, washed with cold methanol and dried under reduced pressure. Yield = 3.17 g, 92%.

^{1}H NMR ($CDCl_3$): δ 12.1 (s, 2H, OH), 8.53 (s, 2H, N=CH), 7.2–7.5 (m, 4H, Ar–H), 7.14 (d, $J = 8$ Hz, 2H, Ar–H), 6.77 (d, $J = 9$ Hz, 2H, Ar–H), 2.04 (s, 6H, Me), 1.24 (s, 18H, ^{t}Bu).

^{13}C{^{1}H} NMR ($CDCl_3$): δ 161.99 (N=C), 159.0, 146.9, 141.8, 137.6, 134.4, 130.6, 129.0, 128.8, 119.0, 117.1, 115.3 (Ar), 34.3 (^{t}Bu), 31.8 (^{t}Bu), 20.2 (Me).

MS (EI$^+$) *m/z*: 532 (M^+), 517 (M^+-CH_3).

IR (CH_2Cl_2) ν cm^{-1}: 3463, 3058, 2959, 1620, 1565, 1488, 1460, 1392, 1362, 1288, 1264, 1243, 1207, 1182, 1135, 1018, 936, 825, 808, 749.

EA for $C_{36}H_{40}N_2O_2$, Calc. C, 81.16; H, 7.57; N, 5.26. Found C, 80.95; H, 7.51; N, 5.32%.

2.2. (*R*)-H_2L^3

(*R*)-(+)-2,2′-Diamino-6,6′-dimethylbiphenyl (1.0 g, 4.7 mmol) and 3,5-dichlorosalicylaldehyde (1.8 g, 9.4 mmol) were dissolved in methanol (25 ml) stirred under reflux for 2 h to produce a bright orange crystalline

solid. The reaction mixture was cooled to −30 °C before the Schiff-base was isolated by vacuum filtration, washed with cold methanol and dried under reduced pressure. Yield = 2.4 g, 93%.

^{1}H NMR ($CDCl_3$): δ 12.85 (s, 2H, OH), 8.42 (s, 2H, N=CH), 7.40 (t, $J = 6$ Hz, 2H, Ar–H), 7.33 (s, 2H, Ar–H), 7.31 (d, $J = 6$ Hz, 2H, Ar–H), 7.15 (s, 2H, Ar–H), 7.12 (d, $J = 6$ Hz, 2H, Ar–H), 2.03 (s, 6H, Me).

^{13}C{^{1}H} NMR ($CDCl_3$): δ 160.2 (N=C), 156.0, 145.9, 137.8, 133.8, 132.9, 130.1, 130.0, 129.4, 123.5, 122.9, 120.7, 115.8 (Ar), 20.2 (Me).

MS (EI$^+$): m/z 556 (M^+).

IR (CH_2Cl_2) ν cm^{-1}: 3069, 2978, 2917, 1615, 1559, 1447, 1377, 1352, 1294, 1264, 1208, 1180, 1101, 1020, 976, 944, 863, 854, 802, 776, 739, 705, 689.

EA for $C_{28}H_{20}N_2O_2Cl_4$, Calc. C, 60.24; H, 3.61; N, 5.02. Found C, 60.00; H, 3.61; N, 4.67%.

2.3. (±)-$Na_2L^1 \cdot x$THF

To a mixture of the Schiff-base H_2L^1 (2.85 g, 4.4 mmol) and sodium hydride (1.06 g, 44.2 mmol) was added THF (30 ml). The reaction mixture was stirred with the system connected to a bubbler. Once hydrogen evolution had stopped the solution was filtered to remove excess sodium hydride and the filtrate was concentrated in vacuo to afford a bright yellow solid. The amount of THF (x) in the material was deduced by careful integration of a ^{1}H NMR spectrum recorded in deuterated pyridine.

^{1}H NMR (d-pyridine): δ 8.30 (s, 2.0H, N=CH), 7.20 (s, 2.1H, Ar–H), 6.68 (bs, 4.0H, Ar–H), 6.25 (bs, 1.9H, Ar–H), 3.64 (m, variable, THF), 1.69 (s, 6.1H, Me), 1.30 (s, 18.2H, ^{t}Bu), 1.30 (m, variable, THF), 1.07 (s, 18.0H, ^{t}Bu).

2.4. (±)-$Na_2L^2 \cdot x$THF

As (±)-$Na_2L^1 \cdot x$THF using the Schiff-base (±)-H_2L^2. Yield = 100%.

^{1}H NMR (d-pyridine): δ 8.57 (s, 2H, N=CH), 7.33–6.66 (m, 12H, Ar–H), 3.66 (m, variable, THF), 1.99 (s, 6H, Me), 1.62 (m, variable, THF), 1.27 (s, 18H, ^{t}Bu).

2.5. (R)-$Na_2L^3 \cdot x$THF

As (±)-$Na_2L^1 \cdot x$THF using the Schiff-base (+)-H_2L^3.

^{1}H NMR (d-pyridine): δ 8.44 (s, 2H, N=CH), 7.22 (s, 2H, Ar–H), 7.15 (d, 2H, Ar–H), 6.88 (t, 2H, Ar–H), 6.86 (s, 2H, Ar–H), 6.47 (m, 2H, Ar–H), 3.45 (m, variable, THF), 1.89 (s, 6H, Me), 1.41 (m, variable, THF).

2.6. [$Mn^{II}L^1$]·THF

The disodium salt $Na_2L^1 \cdot x$THF (580 μmol) and $MnCl_2$ (73 mg, 580 μmol) were stirred in THF (20 ml) for 12 h by which time the metal salt had dissolved and a white precipitate had formed in the dark red solution. The THF was removed in vacuo and the red solid was extracted into pentane and filtered to remove NaCl. The pentane was removed in vacuo and the red solid was recrystallised from THF cooled to −30 °C. Yield = 0.39 g, 88%.

$\mu_{eff} = 5.16$ BM.

MS (EI$^+$) m/z 697 (M^+), 682 (M^+-CH_3), 644 (M^+-Mn).

EA for [$MnC_{48}H_{62}N_2O_3$], Calc. C, 74.88; H, 8.12; N, 3.64. Found C, 74.46; H, 8.23; N, 3.95%.

2.7. [$Mn^{II}L^2$]·2(THF)

The disodium salt $Na_2L^2 \cdot x$THF (654 μmol) and $MnCl_2$ (82 mg, 654 μmol) were stirred in THF (30 ml) for 12 h by which time the metal salt had dissolved and a white precipitate had formed in the bright orange solution. The THF was removed in vacuo and the orange solid was extracted into benzene and filtered to remove NaCl. The benzene was removed in vacuo and the red solid was recrystallised from THF cooled to −30 °C to give small rectangular red crystals. Yield = 0.42 g, 88%.

$\mu_{eff} = 4.98$ BM.

MS (EI$^+$) m/z 585 (M^+), 570 (M^+-CH_3).

EA for [$MnC_{44}H_{54}N_2O_4$], Calc. C, 72.41; H, 7.46; N, 3.84. Found C, 72.86; H, 6.99; N, 4.50%.

2.8. (R)-[$Mn^{II}L^3$]·½(CH_2Cl_2)

The disodium salt $Na_2L^3 \cdot x$THF (297 μmol) and $MnCl_2$ (37 mg, 297 μmol) were stirred in THF (20 ml) for 12 h by which time the metal salt had dissolved and a white precipitate had formed in the bright red solution. The THF was removed in vacuo and the orange solid was extracted into dichloromethane and filtered to remove NaCl. Removal of the dichloromethane in vacuo left a light orange solid. Yield = 0.16 g, 85%.

$\mu_{eff} = 5.26$ BM

MS (FAB$^+$) m/z 609 (M^+).

EA for $MnC_{28.5}H_{19}N_2O_2Cl_5$, Calc. C, 52.37; H, 2.93; N, 4.29. Found C, 52.70; H, 2.95; N, 4.82%.

The orange solid was recrystallised from wet dichloromethane to give orange needles of the complex

$[\{MnL^3\}_2(H_2O)]\cdot 3CH_2Cl_2$ suitable for X-ray crystallography.

2.9. $[Mn^{III}L^1Cl]$

To a vigorously stirred solution of the complex $[Mn^{II}L^1]\cdot$THF (430 mg, 616 μmol) in pentane (20 ml) was added chlorine (6.9 ml, 0.5 equiv.) via a gas-tight syringe. The red solution immediately turned a dark green and a small amount of light green precipitate could be seen in the solution. The solution was quickly filtered and allowed to stir for a further 30 min. The solution was concentrated and cooled (−30 °C) to give a green microcrystalline solid. Yield = 180 mg, 40%.

$\mu_{eff} = 4.40$ BM.

MS (EI^+) m/z 697 (M^+-Cl).

EA for ($MnC_{44}H_{54}N_2O_2Cl$), Calc. C, 72.07; H, 7.42; N, 3.82. Found C, 72.26; H, 7.79; N, 3.16%.

The solid was recrystallised from an acetonitrile/pentane solution in air to give dark brown crystals of the complex $[MnL^1(H_2O)_2]Cl\cdot(C_5H_{12})_{0.25}$ which were isolated and found to be suitable for X-ray diffraction studies.

2.10. $[Mn^{III}L^1I]$

To a vigorously stirred solution of the complex $[Mn^{II}L^1]\cdot$THF (430 mg, 616 μmol) in pentane (20 ml) was added 0.5 equiv. of iodine (78 mg) dissolved in dichloromethane. The red solution immediately changed colour to green/brown and was stirred for 30 min. A brown microcrystalline solid had precipitated from the solution which was filtered and dried in vacuo. Yield = 335 mg, 66%

$\mu_{eff} = 4.25$ BM.

MS (EI^+) m/z 697 (M^+-I).

EA for $(MnC_{44}H_{54}N_2O_2I)_3\cdot CH_2Cl_2$, Calc. C, 62.42; H, 6.46; N, 3.28. Found C, 62.67; H, 6.56; N, 2.78%.

The solid was redissolved in hot pentane and recrystallised to give brown plates of the complex $[MnL^1I]\cdot C_5H_{12}$ which were suitable for X-ray diffraction.

2.11. $[Mn^{III}L^2Cl]$

To a solution of $[MnL^2]\cdot$2THF (110 mg, 187 μmol) in diethyl ether (20 ml) was added chlorine (0.5 equiv., 2.1 ml) via a gas-tight syringe. The solution immediately turned green and was filtered. The solution was stirred for 30 min, concentrated and cooled to −30 °C. A dark green precipitate formed in the solution which was isolated by filtration. The dark green solid was recrystallised from a concentrated dichloromethane solution at −30 °C. Yield = 83 mg, 71%.

$\mu_{eff} = 4.30$ BM.

MS (EI^+) m/z: 585 (M^+-Cl).

EA for $(MnC_{36}H_{38}N_2O_2Cl)\cdot 3CH_2Cl_2$, Calc. C, 53.48; H, 5.06; N, 3.20. Found C, 53.20; H, 4.77; N, 2.78%.

3. Crystallography

Crystals were coated in an inert oil prior transfer to a cold nitrogen gas stream on a Bruker-AXS SMART three circle CCD area detector system equipped with Mo Kα radiation ($\lambda = 0.71073$ Å). Data were collected with narrow (0.3° in ω) frame exposures. Intensities were corrected semi-empirically for absorption, based on symmetry equivalent and repeated reflections (SADABS). Reflection data for all structures were weak and no significant data were found for $2\theta > 45°$. All structures were solved by direct methods (SHELXS) [6] with additional light atoms found by Fourier methods. The asymmetric unit of $[\{Mn^{II}L^3\}_2(H_2O)]\cdot 3CH_2Cl_2$ contains three independent dichloromethane solvent molecules, one of which is disordered. The bond distances in this were constrained to a target value (DFIX) and no further disorder modelling was attempted. The asymmetric unit of $[MnL^1I]\cdot C_5H_{12}$ contains one disordered pentane solvent molecule, the bond distances of which were similarly constrained to a target value (DFIX) with no further modelling attempted. $[MnL^1(H_2O)_2]Cl\cdot(C_2H_{12})_{0.25}$ contains a pentane molecule in its asymmetric unit that was severely disordered across several positions and across an inversion centre. Attempts to fully model this disorder were unsuccessful due to weak data and a consequently low data to parameter ratio. Only one of the positions was modelled and this was assigned an occupancy factor of a quarter which produced the best fit to the experimental data. The anisotropic displacement parameters for each carbon atom in the pentane were constrained to be equal (EADP) to those of C(44). All structures were refined on F^2 values for all unique data. All non-hydrogen atoms were refined anisotropically apart from the disordered dichloromethane and pentane solvent of crystallisation molecules. Isotropic restraints were required for all carbon and nitrogen displacement parameters in $[\{Mn^{II}L^3\}_2(H_2O)]\cdot 3CH_2Cl_2$ due to the poor data/parameter ratio. Hydrogen atoms were constrained with a riding model; U(H) was set at 1.2 (1.5 for methyl groups) times U_{eq} for the parent atom, except for the hydrogen atoms of the water ligands which were found via difference Fourier maps. The bond lengths and angles of these atoms were constrained to a target values (DFIX and DANG). Programs used were Bruker AXS Smart (control) and SAINT (integration) and SHELXTL [7] for structure solution, refinement and molecular graphics.

4. Results and discussion

4.1. Manganese (II) complexes

Meunier [3] and Che [4b] have reported the synthesis of binaphthyl Schiff-base complexes of Mn^{III} by treating the protonated Schiff-base ligand with e.g. manganese acetates and acetylacetonates in alcohols or acetonitrile. We were thus surprised to find that similar reactions of H_2L^n gave mixtures from which pure materials could only be separated with difficulty. Our previous work in early transition metal Schiff-base complex synthesis had employed aprotic techniques [2] and these were successfully applied here.

The hydroxy groups of the H_2L^n ($n = 1$–3) ligands were readily deprotonated by the addition of a solution of the ligand in THF to NaH. Hydrogen was evolved, and $[Na_2(THF)_x][L^n]$ was produced quantitatively. The proportion of THF incorporated into the solid varied slightly at each preparation, but the stoichiometry was readily determined by integration of ^1H NMR spectra recorded in d_5-pyridine. Subsequent reactions of these salts with anhydrous manganese(II) chloride generated bright red solutions which, after extraction into the relevant solvent gave air-sensitive manganese(II) Schiff-base complexes of constitution $[Mn^{II}L^1]\cdot THF$, $[Mn^{II}L^2]\cdot 2THF$, $[Mn^{II}L^3]\cdot\frac{1}{2}CH_2Cl_2$ as bright orange solids. These paramagnetic complexes were characterised by mass spectrometry and elemental analysis. Magnetic moments ranged from 4.98–5.26 BM (cf. 4.25–4.4 for the Mn(III) complexes below).

Single crystals of the chiral non-racemic complex (*R*)-Δ-*cis*-β$_2$-$[\{Mn^{II}L^3\}_2(H_2O)]\cdot 3CH_2Cl_2$ suitable for X-ray diffraction were grown by allowing a solution of pure (*R*)-$[\{Mn^{II}L^3\}_2]\cdot CH_2Cl_2$ in d_2-dichloromethane to evaporate slowly in a poorly-sealed NMR tube. The resultant molecular structure (Table 1) is shown in Fig. 2. The molecule is (necessarily) a homochiral dimer with two μ^2-bridging phenolic oxygen atoms O(11) and O(21), one from each chelate monomer. A weak inter-dimer Cl(21)···Mn(2) [2.816(5) Å] interaction makes this metal centre six-coordinate, but the geometry does not approximate to octahedral or any capped five-coordinate geometry. The N(21)–Mn(2)–O(22) and N(22)–Mn(2)–O(21) angles of 171.0(4)° and 116.8(4)° are similar to those found in trigonal bipyramidal $[MnL^1I]\cdot C_5H_{12}$ [175.4(3)° and 129.7(3)°] (vide infra). The atom Mn(1) is also six-coordinate, by virtue of the addition of an adventitious molecule of water, and is approximately octahedral. As can be seen from the structural parameters selected in Table 2, the two MnL^3 units (e.g. Fig. 3) are very similar. Both adopt the *cis*-β structure, with one phenolic oxygen atom approximately in the plane of the two imine nitrogen atoms and one distinctly out-of-plane.

4.2. Manganese(III) complexes

The manganese(II) complexes of L^{1-3} above formed in situ were oxidised to the manganese(III) compounds on addition of an oxidant (e.g. iodine or chlorine). The solutions immediately changed colour to dark green, and a green solid often precipitated from the reaction mixture. The paramagnetic complexes of composition $[MnL^1I]\cdot(1/3)(CH_2Cl_2)$, $[MnL^1Cl]$, $[MnL^2Cl]\cdot 3(CH_2Cl_2)$ were characterised by mass spectrometry and elemental analysis.

Pure $[MnL^1I]\cdot(1/3)(CH_2Cl_2)$ was recrystallised from pentane to give $[MnL^1I]\cdot C_5H_{12}$, the molecular structure of which is shown in Fig. 4. The complex is a monomer and can be described as a distorted trigonal bipyramid with N(1)–Mn(1)–O(2) [175.4(3)°] as the principal axis.

Table 1
Experimental data for the X-ray diffraction studies

	$[(MnL^3)_2(H_2O)]\cdot 3CH_2Cl_2$	$[MnL^1I]\cdot C_5H_{12}$	$[MnL^1(H_2O)_2]Cl\cdot(C_5H_{12})_{0.25}$
Molecular formula	$C_{59}H_{44}Cl_{14}Mn_2N_4O_5$	$C_{49}H_{66}IMnN_2O_2$	$C_{44.25}H_{61}ClMnN_2O_4$
Formula weight	1491.13	896.88	787.35
Crystal system	monoclinic	triclinic	triclinic
Space group	$P2_1$	$P\bar{1}$	$P\bar{1}$
a (Å)	14.8413(12)	11.483(2)	8.5640(10)
b (Å)	12.1527(12)	13.009(3)	16.2352(15)
c (Å)	18.6686(3)	17.865(4)	17.5287(10)
α (°)		76.654(5)	109.504(2)
β (°)	109.613(2)	79.293(5)	92.382(2)
γ (°)		67.833(5)	97.9570(10)
Cell volume (Å^3)	3171.7(4)	2390.2(8)	2265.1(4)
Z	2	2	2
μ (mm^{-1})	1.039	0.959	0.389
Total reflections	12 897	9692	8988
Independent reflections	6491 ($R_{int} = 0.1101$)	6174 ($R_{int} = 0.0385$)	5795 ($R_{int} = 0.0819$)
R_1, wR_2 [$I > 2\sigma(I)$]	0.0904, 0.1939	0.0693, 0.1487	0.0892, 0.1946

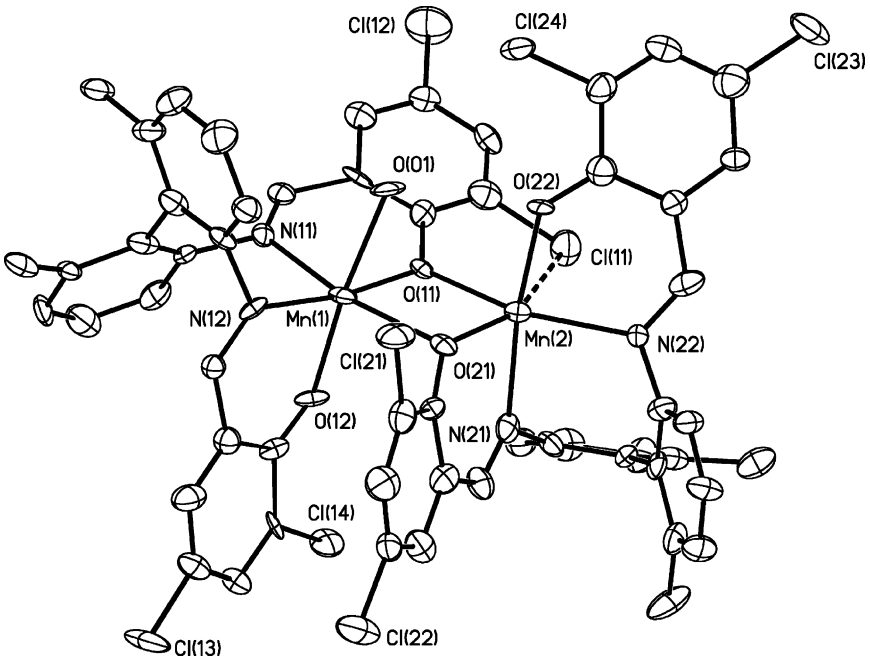

Fig. 2. Thermal ellipsoid plot of the molecular structure of the bimetallic unit in $[\{Mn^{II}L^3\}_2(H_2O)]\cdot 3CH_2Cl_2$.

The angles N(2)–Mn(1)–O(1) and N(2)–Mn(1)–I(1) are 129.7(3)° and 113.8(2)°, respectively. The deviations of the atoms N(1), N(2), O(2) and Mn(1) from their least-squares plane are all less than 0.03 Å, while O(1) is necessarily out-of-plane. The molecule should thus be described as having a *cis*-β structure by analogy with the octahedral cases above. While noting that the sample in this case was racemic, the configuration shown in Fig. 4 is (*S*)-Λ-*cis*-β.

Table 2
Selected bond lengths (Å) and angles (°) for the two fragments of $[\{Mn^{II}L^3\}_2(H_2O)]\cdot 3CH_2Cl_2$

Mn(1) unit		Mn(2) unit	
Bond lengths			
Mn(1)–O(12)	2.036(11)	Mn(2)–O21	2.078(10)
Mn(1)–O(11)	2.140(11)	Mn(2)–O22	2.087(11)
Mn(1)–N(12)	2.179(12)	Mn(2)–O11	2.188(10)
Mn(1)–N(11)	2.239(12)	Mn(2)–N21	2.197(16)
Mn(1)–O(21)	2.291(10)	Mn(2)–N22	2.239(12)
Mn(1)–O(01)	2.282(13)	Mn(2)–Cl11	2.816(5)
Bond angles			
O(12)–Mn(1)–O(11)	100.1(5)	O(21)–Mn2–O22	97.0(5)
O(12)–Mn1–N(12)	84.3(5)	O(22)–Mn2–N22	85.4(5)
O(11)–Mn(1)–N(12)	171.5(5)	O(22)–Mn2–N21	170.0(4)
O(12)–Mn(1)–N(11)	95.0(4)	O(11)–Mn2–N21	97.6(5)
O(11)–Mn(1)–N(11)	84.4(4)	O(22)–Mn2–O11	91.5(4)
N(12)–Mn(1)–N(11)	88.1(4)	N(21)–Mn2–N22	86.5(5)
O(12)–Mn(1)–O(21)	90.2(4)	O(21)–Mn2–N21	82.9(5)
O(11)–Mn(1)–O(21)	83.2(4)	O(21)–Mn2–O11	87.3(4)
N(12)–Mn(1)–O(21)	104.0(4)	O(21)–Mn2–N22	116.8(4)
N(11)–Mn(1)–O(21)	167.2(4)	O(11)–Mn2–N22	155.9(4)
θ [a]	75.3		77.4

[a] The angle between least-squares planes of the biaryl rings.

Crystals of $[Mn^{III}L^1(H_2O)_2]Cl$ were grown from a solution of $[Mn^{III}L^1Cl]$ in acetonitrile/pentane in air. The molecular structure of is shown in Fig. 5, and the cationic unit is shown viewed down the approximate C_2 axis in Fig. 6. The molecule has an approximately octahedral arrangement of the ligating atoms. The phenolic oxygen atoms take a mutually *trans* position in the structure with the imine nitrogen atoms occupying the *cis* sites, as do the oxygen atoms of the two water molecules. The complex $[Mn^{III}L^1(H_2O)_2]Cl$ therefore adopts the rare *cis*-α structure, similar to $[ZrL^1Cl_2]$

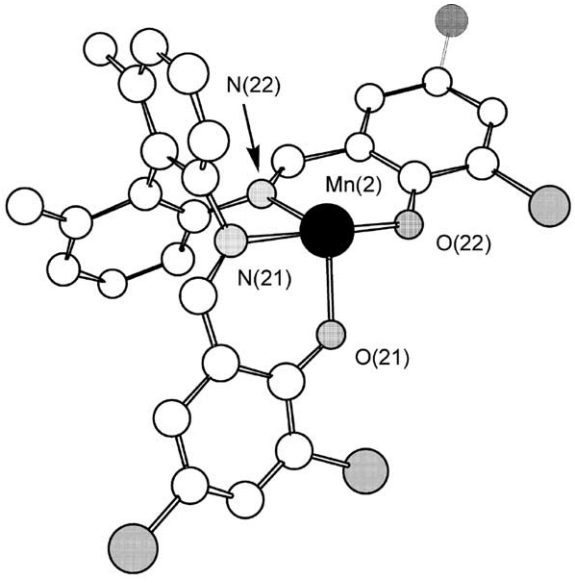

Fig. 3. The $L^3Mn(2)$ unit in $[\{Mn^{II}L^3\}_2(H_2O)]\cdot 3CH_2Cl_2$ showing the *cis*-β orientation. The Mn(1) unit has a very similar structure.

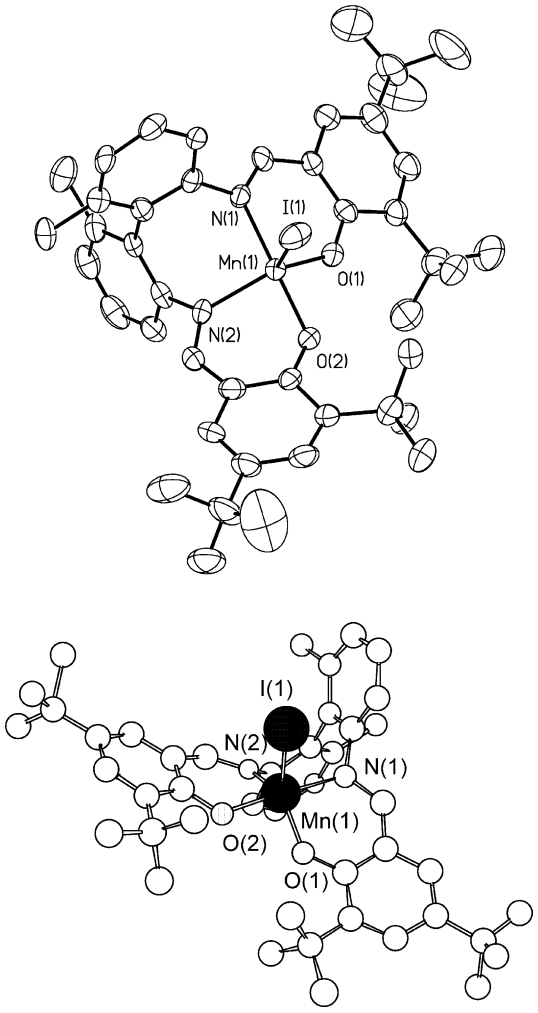

Fig. 4. Thermal ellipsoid and ball and stick views of the molecular structure of [MnL^{1}I]. Selected bond lengths [Å] and angles [°] Mn(1)–O(1) 1.902(6), Mn(1)–O(2) 1.872(5), Mn(1)–N(1) 2.020(6), Mn(1)–N(2) 2.058(6), Mn(1)–I(1) 2.6998(14), O(1)–Mn(1)–O(2) 87.7(2), O(1)–Mn(1)–N(1) 89.1(2), O(1)–Mn(1)–N(2) 129.7(3), O(2)–Mn(1)–N(1) 175.4(3), O(2)–Mn(1)–N(2) 87.2(2), N(1)–Mn(1)–N(2) 92.5(3), O(1)–Mn(1)–I(1) 116.47(18), O(2)–Mn(1)–I(1) 92.41(18), N(1)–Mn(1)–I(1) 91.90(18), N(2)–Mn(1)–I(1) 113.75(19), θ 69.9.

reported previously by our group [2]. Some structural parameters for [MnL^1(H$_2$O)$_2$]Cl and [ZrL^{1}Cl$_2$] are compared in Table 3. As expected, the metal–ligand bonds are shorter for manganese in comparison to zirconium. It is apparent that the arrangement of the ligand L^1 in the manganese complex is less distorted from octahedral geometry than it is for zirconium complex. This is most probably due to a better size match of the Mn(III) ion compared to the larger Zr(IV) ion in the octahedral cavity.

4.3. Catalytic studies

The complexes synthesised above were screened for their effectiveness in the catalysis of the epoxidation of several styrenic alkenes by the I(III) reagent iodosyl benzene PhIO using a standard procedure [4b]. Since very modest turnovers (< 5) for production of epoxides were observed the determination of enantiomeric excess was not persued. It is noteworthy however that GC analysis of the product mixtures invariably showed large amounts of iodobenzene, indicating that the complexes mediate catalase-like decomposition of the PhIO rather than oxygenase-like atom transfer. Meunier has noted that related binaphthyl complexes of manganese catalyse the dismutation of H_2O_2 [3].

5. Conclusions

Several biaryl-bridged N_2O_2 Schiff-base complexes of manganese(II) and (III) have been synthesised and some characterised by X-ray diffraction. As mentioned above, the molecular structure of a binaphthyl-bridged Schiff-base *cis*-β-[Mn^{III}L(acac)] has previously been reported [4b]. It is clear from our work however that despite the conformational restrictions imposed by the atropisomeric biaryl group that there is an unexpectedly fine balance between the *cis*-β or the *cis*-α orientations. While the latter has not hitherto been observed for first row or middle transition metal complexes it is apparent that conversion between diastereomeric forms *cis*-β and *cis*-α with the same sense of helicity (Λ/Δ) may occur. This has important implications for the mechanism of catalysis by this type of chiral-at-metal complex. For example Katsuki's recently reported Co(III) catalysed Baeyer-Villiger oxidation of cyclobutanones [8] may

Table 3
Comparison of selected bond lengths (Å) and angles (°) for the complexes [MnL^1(H$_2$O)$_2$]Cl and [ZrL^{1}Cl$_2$]

	[MnL^1(H$_2$O)$_2$]Cl [X = OH$_2$]	[ZrL^{1}Cl$_2$] [X = Cl]
Bond lengths		
Mn1–O1	1.927(5)	2.410(1)
Mn1–O2	1.921(5)	
Mn1–N1	2.006(7)	2.316(2)
Mn1–N2	2.007(7)	
Mn1–O3	2.031(6)	2.009(1)
Mn1–O4	2.031(5)	
Bond angles		
N(1)–M–N(2)	87.9(3)	75.66(8)
O(1)–M–O(2)	177.0(2)	171.95(8)
X(1)–M–X(2)	89.7(2)	103.56(3)
N(1)–M–X(1)	176.8(3)	161.18(4)
N(2)–M–X(2)	177.4(3)	
O(1)–M–X(1)	90.3(2)	91.62(5)
O(2)–M–X(2)	90.4(2)	
O(1)–M–N(1)	87.1(3)	76.42(6)
θ	69.9	56.1

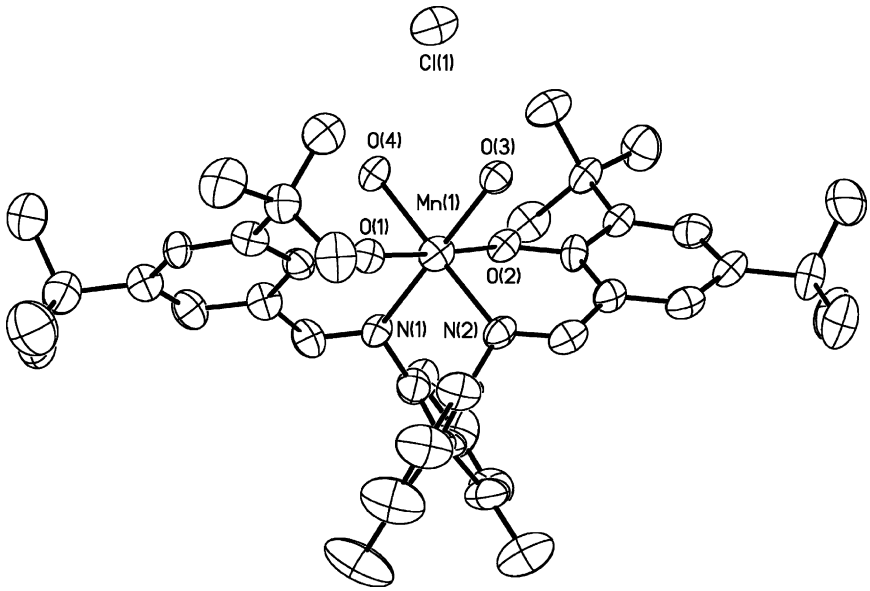

Fig. 5. Thermal ellipsoid plot of $[Mn^{III}L^{1}(H_2O)_2]Cl$.

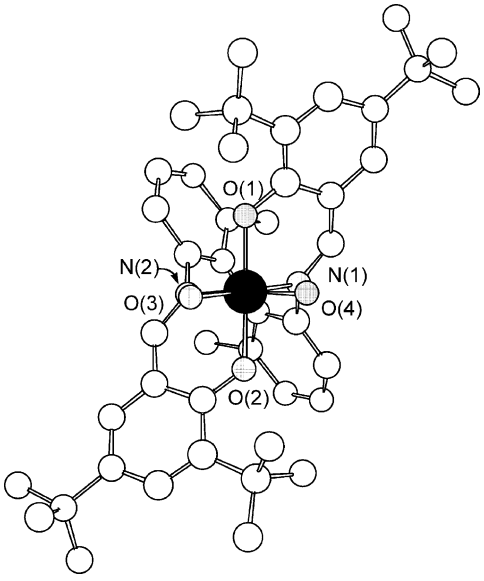

Fig. 6. Molecular structure of $[Mn^{III}L^{1}(H_2O)_2]Cl$ viewed down the approximate C_2 axis.

occur via six-coordinate intermediates of either diastereomeric form, and not necessarily just the *cis*-β isomer.

6. Supplementary material

Crystallographic data for the structural analysis have been deposited with the Cambridge Crystallographic Data Centre, CCDC Nos. 197735–197737. Copies of this information may be obtained free of charge from The Director, CCDC, 12 Union Road, Cambridge, CB2 1EZ, UK (fax: +44-1223-336033; e-mail: deposit@ccdc.cam.ac.uk or www: http://www.ccdc.cam.ac.uk).

Acknowledgements

P.S. thanks EPSRC and GSK for support.

References

[1] (a) E.N. Jacobsen, in: I. Ojima (Ed.), Catalytic Asymmetric Synthesis, VCH, New York, 1993, pp. 159–202;
(b) T. Katsuki, Coord. Chem. Rev. 140 (1995) 189;
(c) T. Katsuki, Adv. Synth. Catal. 344 (2002) 131.
[2] (a) P. Woodman, P.B. Hitchcock, P. Scott, Chem. Commun. (1996) 2735;
(b) P.R. Woodman, C.J. Sanders, N.W. Alcock, P.B. Hitchcock, P. Scott, New J. Chem. 23 (1999) 815;
(c) P.R. Woodman, I.J. Munslow, P.B. Hitchcock, P. Scott, J. Chem. Soc., Dalton Trans. (1999) 4069;
(d) C.J. Sanders, K.M. Gillespie, D. Bell, P. Scott, J. Am. Chem. Soc. 122 (2000) 7132;
(e) P.R. Woodman, N.W. Alcock, I.J. Munslow, C.J. Sanders, P. Scott, J. Chem. Soc., Dalton Trans. (2000) 3340;
(f) K.M. Gillespie, E.J. Crust, R.J. Deeth, P. Scott, Chem. Commun. (2001) 785;
(g) I.J. Munslow, K.M. Gillespie, R.J. Deeth, P. Scott, Chem. Commun. (2001) 1638;
(h) C.J. Sanders, K.M. Gillespie, P. Scott, Tetrahedron: Asymm. 12 (2001) 1055;
(i) P.D. Knight, A.J. Clarke, B.S. Kimberley, R.A. Jackson, P. Scott, Chem. Commun. (2002) 352;
(j) K.M. Gillespie, C.J. Sanders, I. Westmoreland, P. Scott, J. Org. Chem. 67 (2002) 3450;
(k) P.N. O'Shaughnessy, K.M. Gillespie, C. Morton, I. Westmoreland, P. Scott, Organometallics 21 (2002) 4496.
[3] K. Bernardo, S. Leppard, A. Robert, G. Commenges, F. Dahan, B. Meunier, Inorg. Chem. 35 (1996) 387.
[4] (a) C.W. Ho, W.C. Cheng, M.C. Cheng, S.M. Peng, K.F. Cheng, C.M. Che, J. Chem. Soc., Dalton Trans. (1996) 405;
(b) M.C. Cheng, M.C.W. Chan, S.M. Peng, K.K. Cheung, C.M. Che, J. Chem. Soc., Dalton Trans. (1997) 3479;
(c) X.G. Zhou, J.S. Huang, P.H. Ko, K.K. Cheung, C.M. Che, J.

Chem. Soc., Dalton Trans. (2001) 3303;
(d) X.G. Zhou, X.Q. Yu, J.S. Huang, S.G. Li, L.S. Li, C.M. Che, Chem. Commun. (1999) 1789;
(e) X.G. Zhou, J.S. Huang, X.Q. Yu, Z.Y. Zhou, C.M. Che, J. Chem. Soc., Dalton Trans. (2000) 1075;
(f) C.M. Che, H.L. Kwong, W.C. Chu, K.F. Cheng, W.S. Lee, H.S. Yu, C.T. Yeung, K.K. Cheung, Eur. J. Inorg. Chem. (2002) 1456.

[5] (a) U. Knof, A. von Zelewsky, Angew. Chem., Int. Ed. 38 (1999) 302;
(b) H. Brunner, Angew. Chem., Int. Ed. 38 (1999) 302.

[6] (a) G.M. Sheldrick, Acta Crystallogr. A 46 (1990) 467;
(b) G.M. Sheldrick, Acta Crystallogr. D 49 (1993) 18.

[7] G. M. Sheldrick, SHELXTL, 1997, Ver. 5.1, Bruker Analytical X-ray Systems, Madison, WI, USA.

[8] (a) T. Uchida, T. Katsuki, Tetrahedron Lett. 42 (2001) 6911;
(b) A. Watanabe, T. Uchida, K. Ito, T. Katsuki, Tetrahedron Lett. 43 (2002) 4481.